On the Feasibility of Real-Time Mapping of the Geoelectric Field across North America

Open-File Report 2018–1043

U.S. Department of the Interior
U.S. Geological Survey

Cover. View from space of the nighttime lights of the northeastern United States. Aurora light, often seen during magnetic storms, is visible overhead. Image by the National Aeronautics and Space Administration.
(URL for this image: https://www.nasa.gov/multimedia/imagegallery/image_feature_2167.html)

On the Feasibility of Real-Time Mapping of the Geoelectric Field across North America

By Jeffrey J. Love, E. Joshua Rigler, Anna Kelbert, Carol A. Finn,
Paul A. Bedrosian, and Christopher C. Balch

Open-File Report 2018–1043

U.S. Department of the Interior
U.S. Geological Survey

U.S. Department of the Interior
RYAN K. ZINKE, Secretary

U.S. Geological Survey
James F. Reilly II, Director

U.S. Geological Survey, Reston, Virginia: 2018

For more information on the USGS—the Federal source for science about the Earth, its natural and living resources, natural hazards, and the environment—visit https://www.usgs.gov or call 1–888–ASK–USGS.

For an overview of USGS information products, including maps, imagery, and publications, visit https://store.usgs.gov.

Suggested citation:
Love, J.J., Rigler, E.J., Kelbert, Anna, Finn, C.A., Bedrosian, P.A., and Balch, C.C., 2018, On the feasibility of real-time mapping of the geoelectric field across North America: U.S. Geological Survey Open-File Report 2018-1043, 16 p., https://doi.org/10.3133/ofr20181043.

ISSN 2331-1258 (online)

Acknowledgments

We thank S.W. Cuttler, J.A. Herrick, G.M. Lucas, J. McCarthy, and J.L. Slate (U.S. Geological Survey) for reading a draft manuscript. We thank Antti Pulkkinen (NASA) for useful conversations.

Contents

Figures

Conversion Factors

SI to Inch/Pound

Multiply	By	To obtain
	Length	
meter (m)	3.281	foot (ft)
meter (m)	1.094	yard (yd)
kilometer (km)	0.6214	mile (mi)

Abbreviations

Dst	disturbance storm time
E^{x}_{h}	Reference geoelectric field (mV/km) for reference magnetic field of unit amplitude (1 nT)
Hz	hertz (frequency)
nT	nanoTeslas
S/m	siemens (S) per meter (m); electrical conductivity
SWAP	U.S. National Space Weather Action Plan
USGS	U.S. Geological Survey

On the Feasibility of Real-time Mapping of the Geoelectric Field across North America

By Jeffrey J. Love,[1] E. Joshua Rigler,[1] Anna Kelbert,[1] Carol A. Finn,[1] Paul A. Bedrosian,[1] and Christopher C. Balch[2]

Abstract

A review is given of the present feasibility for accurately mapping geoelectric fields across North America in near-realtime by modeling geomagnetic monitoring and magnetotelluric survey data. Should this capability be successfully developed, it could inform utility companies of magnetic-storm interference on electric-power-grid systems. That real-time mapping of geoelectric fields is a challenge is reflective of (1) the spatiotemporal complexity of geomagnetic variation, especially during magnetic storms, (2) the sparse distribution of ground-based geomagnetic monitoring stations that report data in realtime, (3) the spatial complexity of three-dimensional solid-Earth impedance, and (4) the geographically incomplete state of continental-scale magnetotelluric surveys.

Introduction

On March 13, 1989, an intense magnetic storm (for example, Allen and others, 1989) induced Earth-surface geoelectric fields of sufficient strength to interfere with the operation of Québec's high-voltage electric-power-grid system, causing a blackout across the entire Canadian province (for example, Bolduc, 2002). The same storm caused numerous operational problems and anomalies for power-grid systems in the United States, and geomagnetically induced currents damaged a high-voltage transformer at a nuclear-power plant (North American Electric Reliability Corporation, 1990; Barnes and others, 1991). More recently, the magnetic storm of November 6, 2001, caused the failure of electric-power transmission systems in New Zealand (Béland and Small, 2005), and the Halloween magnetic storm of October 29–31, 2003, caused operational failures in Swedish systems (Pulkkinen and others, 2005). Some scenario analyses anticipate that the future occurrence of a rare magnetic superstorm could cause widespread and long-lasting loss of electric power (for example, Kappenman, 2012) and entail significant cost for national economies (for example, Barnes and Van Dyke, 1990; National Research Council, 2008; Eastwood and others, 2017). In light of these events and possibilities, the U.S. Federal Energy Regulatory Commission (2013; Order No. 779) directed the North American Electric Reliability Corporation to assess the vulnerability of United States domestic power-grid systems to geomagnetic disturbance.

Time-dependent maps of ground-level geoelectric fields (for example, Thomson and others, 2009; Love and others, 2014) would enable estimation of geomagnetically induced currents in power-grid networks and thereby support vulnerability assessments of power-grid systems (for example, Molinski, 2002; Samuelsson, 2013; Piccinelli and Krausmann, 2014). Geoelectric maps could also inform operational decision making and management of power-grid systems during geomagnetic storms. There are, however, significant challenges in producing such maps, especially in realtime. Mapping the geoelectric field requires estimates of both the Earth's surface geomagnetic field variation and the Earth's surface electromagnetic impedance. In particular, the accuracy of such modeling is limited by the sparseness of real-time geomagnetic monitoring stations and the incompleteness of magnetotelluric surveys.

The U.S. National Space Weather Action Plan (SWAP) contains directives for Federal government agencies involved with a disparate set of subjects related to space-weather operations, response, and mitigation. One of these directives calls for the Department of the Interior to "report on the feasibility" for providing the Department of Commerce with a "real-time service for geoelectric field maps" (National Science and Technology Council, 2015, Action 5.5.6). This directive, in turn, applies to the U.S. Geological Survey (USGS) and its Geomagnetism Program (Love and Finn, 2011).

[1]U.S. Geological Survey

[2]National Oceanic and Atmospheric Administration

This report was developed to satisfy the SWAP directive. It is also consistent with what the U.S. National Research Council (2013, p. 146) has described as a “critical national need” to develop capabilities for estimating geomagnetically induced currents in power-grid systems; it is consistent with a collaborative study sponsored by Living With a Star Program of the National Aeronautics and Space Administration (NASA) (Pulkkinen and others, 2017); and, in general terms, it is consistent with the goals identified in the USGS Natural Hazards Mission for enhancing observations, fundamental understanding of hazards and their effects, improving assessment products and services, and providing effective situational awareness (Holmes and others, 2013).

Length and Time Scales

In designing a project for mapping geoelectric fields, it is useful to first consider the relevant characteristic length and time scales of power-grid systems themselves. The geomagnetically induced voltage on a power grid can be obtained by point-to-point line integration of the geoelectric field along the length of the grid line between grounding points. The distance between these substations is typically 100 kilometers (km) or so (for example, Horton and others, 2012, table II), and a network can consist of multiple connections stretching across 1,000 km or more. With respect to time scales, we note that the 1989 Hydro-Québec collapse occurred over the course of about 1 minute with tripping of multiple compensators that resulted in system instability (Bolduc, 2002). Electric-utility companies have considered the vulnerability of high-voltage transformers to abnormal heating caused by quasi-direct, geomagnetically induced currents with durations from about 100 seconds to about 10,000 seconds (about 10^{-2} to 10^{-4} hertz [Hz]) (for example, North American Electric Reliability Corporation, 2014a; Pulkkinen and others, 2017).

Motivation for Parameterized Induction

It is tempting to consider continental-scale mapping of geoelectric fields through straightforward interpolation of data acquired from geoelectric observatories. In fact, long-term geoelectric field monitoring is maintained at only a few locations around the world (for example, Fujii and others, 2015), and data from these stations are useful for validating geoelectric estimation methods. However, because of the complexity of solid-Earth conductivity structure, a geoelectric field induced at one location can differ significantly from that induced less than a hundred kilometers away (for example, McKay and Whaler, 2006; Bedrosian and Love, 2015). This means that accurate mapping of geoelectric fields by interpolation of direct measurements would require a very dense network of geoelectric observatories. Unfortunately, it is relatively difficult to operate geoelectric monitoring systems for long durations of time (for example, Ferguson, 2012). A more practical approach for mapping of geoelectric fields would utilize an empirical parameterization of induction (for example, Bonner and Schultz, 2017; Kelbert and others, 2017; Weigel, 2017)—this amounts to muliplication in the frequency domain or convolution in the time domain of a real-time map of horizontal-component geomagnetic variation, derived from ground-level magnetometer data, with a map of the Earth’s surface impedance, derived from magnetotelluric survey data. In what follows, we summarize some of the technical issues, challenges, and opportunities of this approach for operational mapping of geoelectric fields in realtime.

Geomagnetic Monitoring

Magnetometer stations are operated by a variety of institutes for a variety of purposes (for example, Love, 2008). Some of these stations are full-fledged observatories and are, as such, dedicated to the long-term acquisition of accurate magnetometer time series (for example, Rasson and others, 2011); other stations are simpler variometers, for which acquired time series are not necessarily calibrated for absolute accuracy. Many observatory institutes “adjust” their real-time data so that they have a rough calibration. Often, this is a rotation that compensates for magnetometer orientation defined by the local magnetic meridian (the deviation from geographic north is declination); many variometer institutes do not report magnetometer orientation. Some magnetometers are operated with high levels of temporal continuity, whereas others are operated more intermittently. Data from only a subset of the world’s magnetometer stations are available in what might be considered “near-realtime.” Improving ground-level geomagnetic monitoring is an important goal of the SWAP (National Science and Technology Council, 2015, Action 6.2.1), one that would bring significant benefit to the space-weather community but which also comes with significant challenges (for example, Love and Finn, 2017).

With respect to North America, inspection of the INTERMAGNET (www.intermagnet.org; for example, Love and Chulliat, 2013) and SuperMAG (http://supermag.jhuapl.edu; Gjerloev, 2009) databases for 1-second holdings identified data for January 2015 from about 45 stations in Canada, including observatories operated by Natural Resources Canada (NRCan) (Lam, 2011) and variometers that are parts of the AUTUMN (Connors and others, 2009), AUTUMNX (Connors and others, 2016), CARISMA (Mann and others, 2008), and MACCS (Engebretson and others, 1995) projects; 15 stations in the continental United States, including observatories operated by the USGS (Love and Finn, 2011) and variometers that are part of the McMac project (Chi and others, 2013); and 10 stations in Alaska, including observatories operated by the USGS and variometers that are part of the GIMA project (Wilkinson and Heavner, 2006). The geographic distribution of these stations is far from uniform, and the distance between many of them exceeds 1,000 km. Data from all the observatories operated by the USGS are available within about 15 minutes of acquisition, either directly from the USGS or through INTERMAGNET; NRCan data are available to selected users, including the USGS, National Oceanic and Atmospheric Administration, Space Weather Prediction Center, and the U.S. Air Force in near-realtime, though only after a 1-day delay through INTERMAGNET; data from the variometer stations are available on a range of schedules, from a few minutes up to a day or so after acquisition.

Geomagnetic Variation

Geomagnetic field variation is a superposition of numerous signals generated by source electric currents that are both above the Earth's surface and within the Earth's interior. So, for example, although magnetic storms have their source currents in the Earth's ionosphere and magnetosphere, they induce telluric currents in the Earth's interior, and these, in turn, generate magnetic fields that contribute to the totality of the field measured at the surface. During periods of solar-terrestrial quiescence, quasi-periodic geomagnetic variation is sustained by tides in the ocean and ionosphere (for example, Matsushita, 1967). Geomagnetic variation, such as that realized at a particular geographic site, encompasses a wide range of frequencies (periods) (for example, Olsen, 2007).

Ground magnetometers are used to define the time evolutionary phases of magnetic storms (for example, Nishida, 1978; Loewe and Prölss, 1997). Many of these commence suddenly, with the arrival at Earth of interplanetary shocks driven by coronal-mass ejections (for example, Tsurutani and Gonzalez, 1997). Storm commencements and related intrastorm impulses (for example, Joselyn and Tsurutani, 1990) are seen globally in ground-magnetometer time series as abrupt changes in geomagnetic field across a broad range of latitudes with time scales ranging from seconds (Araki and others, 1997) to a few minutes (for example, Araki and others, 2004). After storm commencement, geomagnetic disturbance is roughly organized by geomagnetic latitude (for example, Ngwira and others, 2013; Woodroffe and others, 2016). Storm main-phase is characterized by the reduction in low-latitude intensity that is generated by an intensification of the magnetospheric ring current (for example, Gonzalez and others, 1994; Cowley, 2007). During a magnetic substorm, abrupt rearrangements of the plasma and fields in the Earth's magnetotail divert electric currents into and out of the high-latitude ionosphere (for example, McPherron, 1991; Kamide and others, 1998). These substorm currents can generate both auroral light and localized ground-level geomagnetic disturbance. During an intense magnetic storm, the auroral oval and associated geomagnetic disturbance can drift down to lower latitudes (Nagata, 1950), such as those of the continental United States.

Small-scale ionospheric currents at a height of about 100 km will, by geometric attenuation, generate ground-level geomagnetic disturbance having horizontal length scales exceeding 100 km. This expectation is supported by analyses of data acquired from closely spaced, high-latitude magnetometers: geomagnetic disturbance with periods longer than 10 seconds has a horizontal-length scale greater than about 200 km (for example, Watermann and others, 2006; Ngwira and others, 2015). Ground-level substorm disturbance typically lasts for an hour or two (for example, Akasofu, 1964), interspersed by quieter periods of a few hours (for example, Borovsky and others, 1993), but occasionally, long bouts of substorm disturbance can persist for days or a week or more (for example, Tsurutani and others, 2004).

Although these general observations can guide our project for mapping geomagnetic variation, we also recognize that the spatiotemporal details of geomagnetic disturbance (for example, Valdivia and others, 1999; Pulkkinen and others, 2006) are unique for each storm. Some storms exhibit complicated geomagnetic disturbance, whereas for others it can be relatively simple. Sometimes, over the course of a storm, disturbance can evolve from simple to complex and back to simple. Indeed, it is sometimes said that "if you have seen one storm, you have seen one storm" (Friedel and others, 2002, p. 266). Furthermore, physics-based models of the coupled solar-wind-magnetospheric-ionospheric system cannot yet accurately predict the idiosyncratic, storm-time, spatiotemporal details of ground-level geomagnetic disturbance, especially at mid- and auroral-zone latitudes (for example, Pulkkinen and others, 2013; Rastätter and others, 2013; Tóth and others, 2014).

A straightforward, empirical demonstration of some of the challenges faced in mapping the storm-time geomagnetic field is given in figure 1, where we plot north-south (B_x) disturbance during the Halloween storm of October 2003 as recorded with 1-minute sampling by magnetometers at two observatories, Ottawa (OTT, Ontario, Canada) and Fredericksburg (FRD, Virginia, United States), that are on nearly the same magnetic longitude but different magnetic latitudes. From this figure, we see that the time series are similar for about 2 hours during the initial phase of the storm, but afterward, large-amplitude variation with time scales shorter than a couple of hours are not well correlated for the remaining duration of the storm.

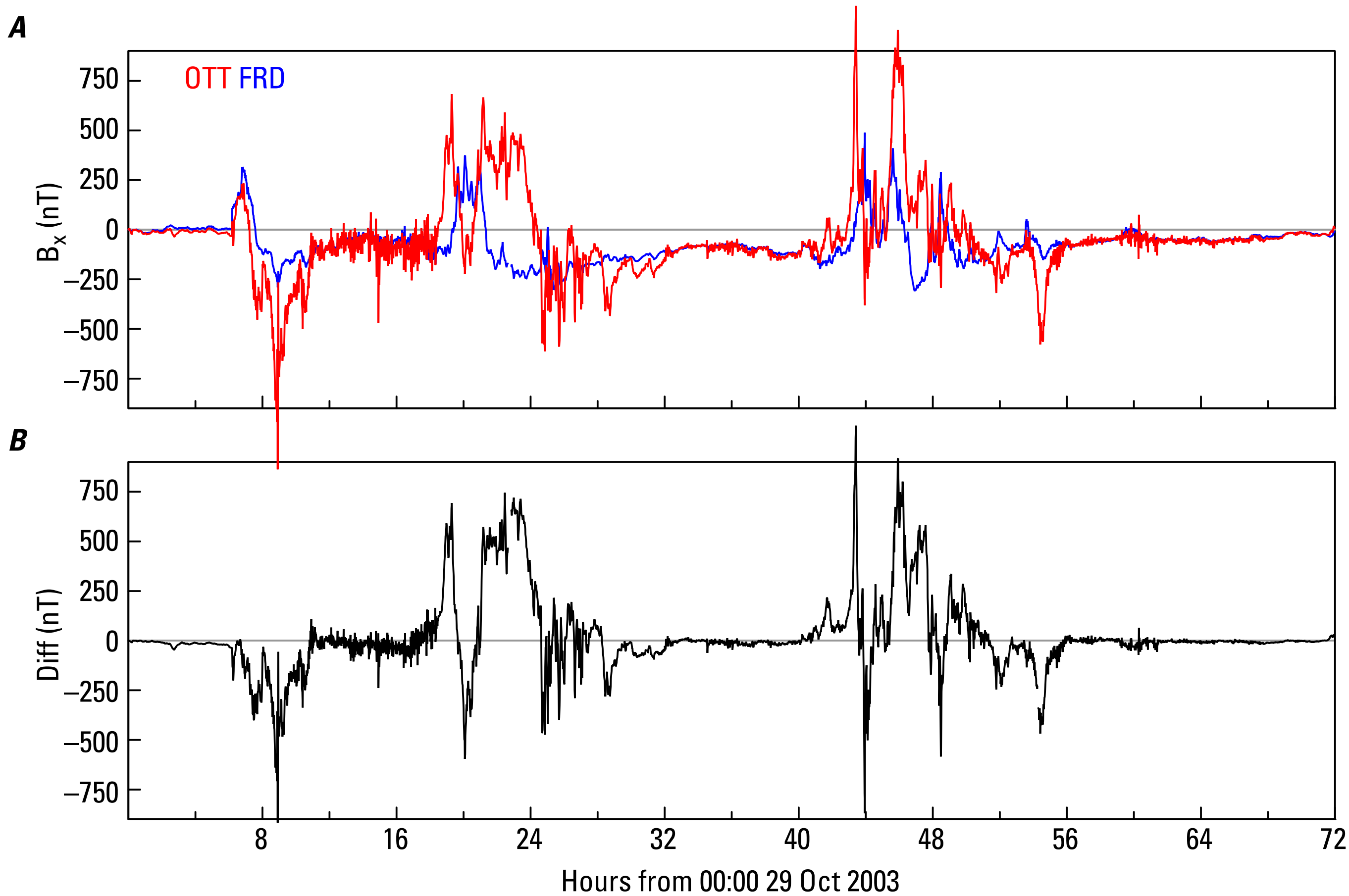

Figure 1. Comparison of (*A*) 1-minute north-south B_x geomagnetic variation time series recorded at the Ottawa (red, OTT, magnetic 55.37°N, 355.88°E) and Fredericksburg (blue, FRD, magnetic 48.14°N, 353.93°E) observatories during the Halloween storm of October 29–31, 2003, and (*B*) the difference between the OTT and FRD time series. These observatories are separated by 814 kilometers. B_x, in nanoteslas; Difference, in nanoteslas. FRD data from Love and Bedrosian, 2018, fig. 2.

Mapping Geomagnetic Variation

Careful consideration needs to be given for the methods used to construct maps of geomagnetic variation with the data that are presently available from ground-based magnetometer stations. Simple, nearest-neighbor and two-dimensional interpolation methods do not use well-defined correlation lengths, and the resolution of the model's field is not better than the spacing of stations (too sparse). Statistical interpolation, such as kriging (for example, Armstrong, 1998), is somewhat better, but it requires prior understanding of correlation lengths. Better are methods based on physically realistic assumptions. Specifically, one can assume that the field below the ionosphere and above the Earth's surface is free of currents and solve for the magnetic field potential in the region. With this, it is conventional to construct maps of geomagnetic variation using regularized least-squares fitting (for example, Menke, 2012) of mathematical basis functions to magnetometer data. Three types of basis functions are in common use: for global mapping, spherical harmonics (for example, Winch, 1981); for regional mapping, spherical cap (for example, Haines and Torta, 1994); and spherical elementary current systems (SECS) (for example, Amm and Viljanen, 1999; Weygand and others, 2011). Development of an operational capability for near-realtime mapping of geomagnetic variation (for example, Rigler and others, 2014) using SECS algorithms (for example, Pulkkinen and others, 2003) is part of an ongoing interagency collaborative project between the USGS, NASA, and the National Oceanic and Atmospheric Administration (National Science and Technology Council, 2015, Action 5.5.6).

In assessing the errors in SECS maps of geomagnetic variation over North America, it is helpful to examine two related analyses. Using data recording a magnetic storm of modest intensity (maximum -Dst = 101 nanoteslas [nT]; where Dst refers to disturbance storm time) acquired from a relatively dense magnetometer network operated in Scandinavia, Pulkkinen and others (2003) found misfit errors in estimates of local geomagnetic variation of about 10 percent (approximately 100 nT) during disturbance (their fig. 9);

misfit errors in their estimates of the time derivative of the field exceed a factor of 2 (their fig. 10). Using data recording relatively quiescent conditions (maximum -Dst = 55 nT) acquired from a sparse distribution of observatories in Northern Canada and Alaska, McLay and Beggan (2010) found misfit errors in estimates of local geomagnetic variation of approximately 50 nT but also occasionally more than 300 nT, or an amount comparable to the amplitude of variation in the field itself (see their fig. 2, and compare with our fig. 1). These results are sobering, and they are cause for caution in concluding that geomagnetic variation can be easily mapped. They indicate a need for systematic assessment of uncertainties in the results from such methods.

Solid Earth Electrical Conductivity and Diffusion

The electrical conductivity of the Earth has a complicated spatial distribution, this being reflective of the Earth's geological history and tectonic structure. The most complicated conductivity structure is concentrated in the Earth's crust, which extends to a depth of approximately 20–50 km in North America (for example, Bally and Palmer 1989; Chulick and Mooney, 2002); over lateral spatial scales of interest to the power-grid industry (several kilometers to thousands of kilometers), crustal conductivity spans at least 4–6 orders of magnitude—from highly conducting to effectively insulating (or resistive)—depending on a myriad of factors, including mineralogy, partial melt, water and aqueous fluid content, clay content, volatile content, porosity, and so forth (for example, Yoshino, 2011; Evans, 2012). Deeper down, the continental lithosphere (extending to depths of approximately 50 to approximately 200 km) followed by the asthenosphere (below the lithosphere) extend down to the upper transition zone boundary at 410 km depth, and these have complicated conductivity structure; indeed, even the Earth's upper to mid-mantle down to 1,200 km or so is known to exhibit significant spatial structure spanning several orders of magnitude (for example, Kelbert and others, 2009).

Time-dependent geomagnetic field variation, such as that generated in geospace and measured at the Earth's surface, propagates into the Earth's interior in a manner that is, essentially, diffusive for the frequency (period) range of interest (for example, Stratton, 1941, chap. 5; Weidelt and Chave, 2012). The Earth's structure affects the characteristic length scale across which these electromagnetic signals are attenuated in the Earth's interior; the diffusive "skin depth" is proportional to the square root of the period of geomagnetic variation and inversely proportional to the square root of the conductivity. For example, for bulk conductivity of 10^{-3} siemens per meter (S/m), which might correspond to dry continental craton, and for a 240-second (4-minute) electromagnetic variation, the diffusive length scale is about 250 km; correspondingly, for bulk conductivity of 10^{-1} S/m, which might correspond to a sedimentary basin, the diffusive length scale is about 25 km. In other words, a 240-second electromagnetic variation can plumb the depths of continental crust and even the continental lithosphere. We note that these scales of several tens to several hundred kilometers also correspond, very approximately, to the typical lateral distance between neighboring electric-power-grid substation ground points in North America. Longer periods of interest, out to a few hours, can propagate as deep as a thousand kilometers.

Magnetotelluric Surveys

Magnetotellurics is a passive geophysical exploration method for estimating the electrical conductivity structure of the Earth's crust, lithosphere, and upper mantle (for example, Unsworth, 2007). Magnetotelluric surveys are performed for purposes of geothermal and mineral exploration, for the study of earthquake and volcano hazards, and for fundamental geophysical research (for example, Ritter, 2007). A survey of a given geographic region is accomplished through temporary deployment of electromagnetic sensors (magnetometers and grounded electrodes) with which simultaneous measurement is made of natural geomagnetic variation and geoelectric field variation at the Earth's surface (for example, Simpson and Bahr, 2005; Ferguson and others, 2012).

In the United States, the National Science Foundation's EarthScope program (Williams, and others, 2010) has, since 2006, supported a magnetotelluric survey that has covered about half of the continental United States to date (Schultz, 2010). The EarthScope magnetotelluric survey is being accomplished with a transportable set of measurement systems, installed at a quasi-regular 70-km spacing and operated for about 2–4 weeks at each site. The EarthScope impedance tensors can be obtained from the Data Management Center of the Incorporated Research Institutions for Seismology (http://ds.iris.edu/ds/products/emtf; Kelbert and others, 2011). The tensors (Schultz and others, 2006–2018) are roughly limited to a frequency band of 10^{-4} to 10^{-1} Hz (10 to 10,000 seconds). In a separate, smaller project, the USGS performed a magnetotelluric survey of the Florida peninsula in 2015 consistent with EarthScope magnetotelluric protocols. In Canada, the Natural Sciences and Engineering Research Council has supported magnetotelluric surveys of southern Canada through its Lithoprobe program (for example, Hammer and others, 2011), though these surveys have not been performed on a broad geographic scale like that made through EarthScope.

Impedance and Models of Earth Conductivity

It is conventional to summarize the Earth-surface relation between the geomagnetic field and the induced geoelectric field in terms of a complex-valued, frequency-dependent impedance tensor. Physically, impedance is determined by the conductivity structure of the Earth's interior (for example, Weidelt and Chave, 2012). An empirical impedance tensor can be constructed (for example, Egbert, 2007a; Chave, 2012) by Fourier transforming the magnetotelluric time series using a regularized least-squares fitting method (for example, Menke, 2012). Empirical impedance tensors can, in turn, be inverted for models of Earth conductivity structure (for example, Egbert, 2007b; Rodi and Mackie, 2012) using regularized nonlinear inverse methods along with standard numerical packages (for example, Kelbert and others, 2014). Earth conductivity models obtained by magnetotelluric inversion methods are usually parameterized in terms of either finite-difference or finite-elements computational grids (for example, Kelbert and others, 2014), and these usually show that Earth conductivity is three-dimensional (3D) in structure (for example, Hermance, 2011).

Conductivity models obtained using the EarthScope magnetotelluric tensors inform fundamental understanding of North American geology and tectonic history (for example, Bedrosian and Feucht, 2014; Meqbel and others, 2014; Yang and others, 2015; Bedrosian 2016; Murphy and Egbert, 2017). They also provide us with important insight on the feasibility of mapping geoelectric fields. In particular, synthetic analyses of the EarthScope magnetotelluric impedance tensors show that some geographic regions would realize significant site-to-site differences in induced geoelectric fields during magnetic storms, sometimes as large as 2 orders of magnitude over distances of about 100 km, whereas other regions would realize relatively uniform geoelectric fields over broad areas (Bedrosian and Love, 2015). Beyond certain rules of thumb, and without a significant computational cost, error estimates on model impedance can be obtained by comparing the modeled magnetotelluric impedances with local empirical impedances coming from auxiliary finer scale survey installations.

In figure 2, we show a map of synthetic geoelectric amplitudes (scalar impedances) that would be induced by spatially uniform north-south geomagnetic variation having unit amplitude (1 nanotesla [nT]) and varying in time as a sinusoid with a period of 240 seconds. Geographic differences in the induced geoelectric fields are due solely to geological and deeper tectonic structure. Generally speaking, synthetic amplitudes are large above the resistive igneous craton, such as in northern Minnesota (MN), and small above conductive sedimentary rocks, such as in Florida (FL). Significant differences in amplitude between neighboring northern Minnesota sites are consistent with a complex 3D subsurface conductivity structure (for example, Yang and others, 2015; Bedrosian, 2016), including a failed continental rift that convulsed the continent 1.1 billion years ago (for example, Stein and others, 2016). The spatial resolution of maps such as this are, of course, limited by the station spacing of the EarthScope magnetotelluric survey; resolving smaller scale conductivity features is possible, but it would require a denser magnetotelluric survey.

Calculation of Geoelectric Fields from Earth Impedance

The geoelectric field at the Earth's surface can be obtained by convolving a map of horizontal-component geomagnetic variation with a map of the Earth's surface impedance. This convolution can be performed, for a given location, in the frequency domain, by applying an inverse discrete Fourier transform to the geomagnetic variation time series (for example, Bonner and Schultz, 2017; Weigel, 2017), or in the time domain, after converting the local impedance to a discrete impulse response function (for example, Marti and others, 2014; Kelbert and others, 2017). Analyses using these methods show that peak geoelectric field variation can be estimated with an error of within 15 percent (Kelbert and others, 2017).

Realistic 3D Versus Simplistic 1D Models of Earth Conductivity

In contrast to analyses based on magnetotelluric surveys, some studies of storm-time geoelectric fields (for example, Boteler, 1997; Pulkkinen and others, 2008; Gannon and others 2012; Wei and others, 2013; Marti and others, 2014; North American Electric Reliability Corporation, 2014b; Viljanen and others, 2014; Boteler and Pirjola, 2017; Torta and others, 2017; Winter and others, 2017) have been based on impedances calculated from simplistic one-dimensional (1D) or 1D piecewise assemblies of regional depth-dependent conductivity profiles estimated indirectly and qualitatively from geological and geophysical information (for example, Ferguson and Odwar, 1997; Ádám and others, 2012; Fernberg, 2012; Blum and others, 2015). We also note that the geoelectric field time series that Natural Resources Canada makes available on their website are obtained using 1D impedances (Trichtchenko and others, 2016).

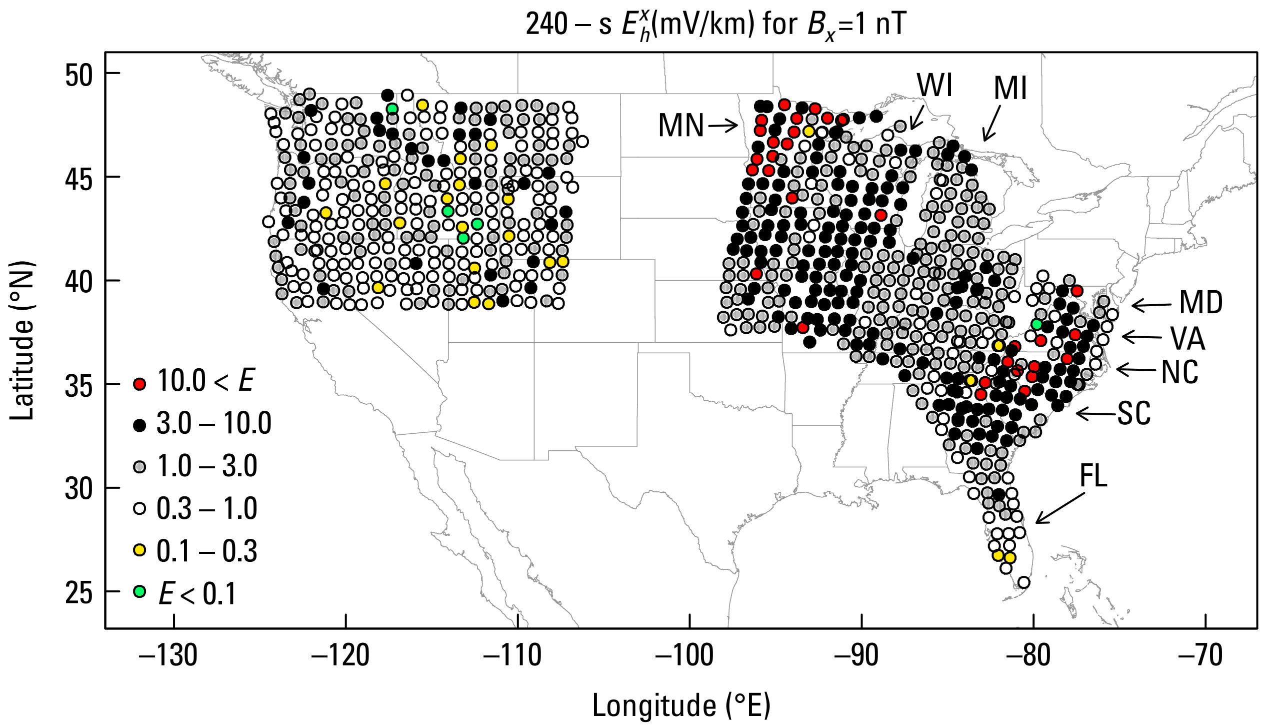

Figure 2. Map showing synthetic geoelectric amplitudes E^x_h (scalar impedances) at EarthScope and U.S. Geological Survey sites for north-south geomagnetic induction B_x with a sinusoidal amplitude of 1 nanotesla and a period of 240 seconds. (second, s; millivolts per kilometer, mV/km). Modified from Love and Bedrosian, 2018, fig. 4A.

Independent of the details of these analyses and their accuracy, because induction occurs within a continuous volume, for sites above 3D Earth structure, a 1D impedance will not generally be a good approximation of the corresponding impedance—the amplitude, polarization, and phase of the geoelectric fields induced in a realistic 3D structure will differ, often significantly, from those induced in an idealized 1D structure (for example, McKay and Whaler, 2006; Bedrosian and Love, 2015; Bonner and Schultz, 2017; Kelbert and others, 2017; Weigel, 2017). Furthermore, piecewise induction of geoelectric fields in piecewise 1D impedances cannot resemble the induction of geoelectric fields from a fully 3D impedance. For these reasons, it would be worthwhile to reexamine the accuracy of geoelectric field results derived from qualitative 1D impedances.

Interpolation and Validation of Geoelectric Field Estimates

To map geoelectric fields by parameterized induction, two alternative methods are available. The first might be described as physically motivated: a plausible 3D conductivity model is constructed from the magnetotelluric impedance tensors, and from this, and for a chosen geographic location, the model magnetotelluric impedance is calculated as a forward problem (for example, Avdeev, 2007; Weiss, 2012). The model impedance can then be convolved with a geomagnetic field time series taken from a variation map to obtain a map of the geoelectric field as a function of time. The second method is more computationally convenient, though it probably requires good survey coverage for a chosen geographic location. Here, a closely spaced set of magnetotelluric impedance tensors are convolved with geomagnetic time series. The resulting geoelectric time series are interpolated to a chosen location (for example, Bonner and Schultz, 2017). A comparison of the two computational methods has not yet been performed.

Maps of storm-time geoelectric fields obtained by parameterized induction are likely to show localized areas of complexity that is the result of a combination of spatially complicated geomagnetic disturbance and spatially complicated impedance. An important spot-check on the accuracy of the estimated geoelectric fields can be made by comparing them directly against measured data, such as those now being acquired at the USGS Boulder magnetic observatory in Colorado (Blum and others, 2017); residual differences between measured and modeled geoelectric fields can be continuously updated and made available in realtime. Comparisons with geoelectric field measurements obtained with temporary magnetotelluric deployments or from longer operating observatories provide a valuable validation opportunity for geoelectric field modeling (for example, Bonner and Schultz, 2017; Kelbert and others, 2017; Weigel, 2017).

Implementation

Geoelectric maps, be they in realtime or otherwise, can be provided on a spatial grid (such as latitude-longitude). To minimize quantization error, geoelectric values would sensibly be reported with a grid spacing that is finer than that afforded by measured data. Alternatively, the geomagnetic mapping algorithms could be provided along with gridded estimates of Earth impedance so that a user agency could, with real-time geomagnetic data streams, produce (locally) their own maps of geoelectric field. In some cases, it might be useful to use a finely spaced grid in regions where it is required by auroral-zone concentration of geomagnetic variation and localized complexity in Earth impedance. As new magnetotelluric data become available, gridded estimates of Earth impedance might be periodically updated. To facilitate reproducibility, data, models, and algorithms should be referenced by version numbers, digital object identifiers, and metadata.

Applications

For direct calculation of the geomagnetically induced current at transformer-ground point in a power-grid network, two quantities are needed (for example, Pirjola, 2002; Horton and others, 2012; North American Electric Reliability Corporation, 2013): (1) the network admittance, which is a function of ground-point resistivities that can be directly measured (for example, Gill, 2009, chap. 11), and (2) the geomagnetically induced voltages on the network lines between the ground points, which can be obtained by line integration of the geoelectric fields obtained by the empirical mapping methods discussed here. Real-time estimation of geomagnetically induced currents could support real-time assessments of power-grid systems, which have, so far, relied on 1D Earth impedances (for example, Boteler and others, 2007; Marti and others, 2013). Geoelectric maps of historical magnetic storms would inform the design of power-grid systems that are resilient to geomagnetic disturbance.

Gap Summary

The routine mapping of geomagnetic variation over North America certainly presents significant practical challenges. Additional magnetometer stations (National Science and Technology Council, 2015, Action 5.3.6), supported by modest amounts of dedicated support, would certainly improve what is expected to be the relatively poor spatial resolution of real-time geomagnetic variation maps. These stations would sensibly be concentrated between about 45° and 65° north magnetic latitude, a zone that experiences intense and spatially complex storm-time disturbance and that encompasses several large North American urban centers (New York, Chicago, Washington, Philadelphia, Boston, Toronto, and others). The resolution of the geomagnetic variation maps can also be improved by incorporating additional physics that might be brought to the modeling of the magnetometer data; most promisingly, using assimilative methods (for example, Schunk and others, 2004; Kihn and Ridley, 2005; Qian and others, 2014) and accommodating spherical-Earth geometries (for example, Kelbert and others, 2009; Sun and others, 2015).

The other glaring need is completion of U.S. magnetotelluric surveys (National Science and Technology Council, 2015, Action 5.5.5)—only about half of the continental United States has been covered. Very importantly, recent survey work has included the northeastern United States, a region that includes major metropolitan centers and substantial electric-power-grid infrastructure and is situated on top of old and complicated geological and tectonic structures and at latitudes where geomagnetic disturbance can be intense. By 2018, it is anticipated that the EarthScope magnetotelluric survey will have been completed across the Dakotas and Nebraska. Funding has not yet been secured to complete the survey across the southwestern and south-central United States, though this would certainly be extremely useful. Extending the magnetotelluric survey into southern Canada would also facilitate real-time mapping of geoelectric fields of importance for assessing magnetic-storm interference on integrated North American power-grid networks.

References Cited

Ádám, A., Prácser, E., and Wesztergom, V., 2012, Estimation of the electric resistivity distribution (EURHOM) in the European lithosphere in the frame of the EURISGICWP2 project: Acta Geodaetica et Geophysica Hungarica, v. 47, no. 4, p. 377–387, accessed January 31, 2018, at https://doi.org/10.1556/AGeod.47.2012.4.1.

Akasofu, S.-I., 1964, The development of the auroral substorm: Planetary and Space Science, v. 12, no. 4, p. 273–282, accessed January 31, 2018, at https://doi.org/10.1016/0032-0633(64)90151-5.

Allen, Joe; Sauer, Herb; Frank, Lou; and Reiff, Patricia, 1989, Effects of the March 1989 solar activity: Eos Transactions American Geophysical Union, v. 70, no. 46, p. 1479, 1486–1488, accessed January 31, 2018, at https://doi.org/10.1029/89EO00409.

Amm, O., and Viljanen, A., 1999, Ionospheric disturbance magnetic field continuation from the ground to the ionosphere using spherical elementary current systems: Earth Planets Space, v. 51, p. 431–440, accessed January 31, 2018, at https://doi.org/10.1186/BF03352247.

Araki, T., Fujitani, S., Emoto, E., Yumoto, K., Shiokawa, K., Ichinose, T., Luehr, H., Orr, D., Milling, D.K., Singer, H., Rostoker, G., Tsunomura, S., Yamada, Y., and Liu, C.F., 1997, Anomalous sudden commencement on March 24, 1991: Journal of Geophysical Research, v. 102, no. A7, p. 14075–14086, accessed January 31, 2018, at https://doi.org/10.1029/96JA03637.

Araki, T., Takeuchi, T., and Araki, Y., 2004, Rise time of geomagnetic sudden commencements—Statistical analysis of ground geomagnetic data: Earth Planets Space, v. 56, no. 2, p. 289–293, accessed January 31, 2018, at https://doi.org/10.1186/BF03353411.

Armstrong, Margaret, 1998, Basic linear geostatistics: Berlin, Germany, Springer-Verlag, 153 p.

Avdeev, D.B., 2007, EM modeling, forward, *in* Gubbins, David, and Herrero-Bervera, Emilio, eds., Encyclopedia of geomagnetism and paleomagnetism: Dordrecht, The Netherlands, Springer, p. 215–218, accessed January 31, 2018, at https://doi.org/10.1007/978-1-4020-4423-6.

Bally, A.W., and Palmer, A.R., 1989, The geology of North America—An overview: Boulder, Colo., Geological Society of America, 629 p., accessed January 31, 2018, at https://doi.org/10.1130/DNAG-GNA-A.

Barnes, P.R., Rizy, D.T., McConnell, B.W., Tesche, F.M., and Taylor, E.R., Jr., 1991, Electric utility industry experience with geomagnetic disturbances: Oak Ridge National Laboratory, report no. ORNL–6665, 78 p.

Barnes, P.R., and Van Dyke, J.W., 1990, Economic consequences of geomagnetic storms (a summary): IEEE Power Engineering Review, v. 10, no. 11, p. 3–4, accessed January 31, 2018, at https://doi.org/10.1109/39.60450.

Bedrosian, P.A., 2016, Making it and breaking it in the Midwest—Continental assembly and rifting from modeling of EarthScope magnetotelluric data: Precambrian Research, v. 278, p. 378–361, accessed January 31, 2018, at https://doi.org/10.1016/j.precamres.2016.03.009.

Bedrosian, P.A., and Feucht, D.W., 2014, Structure and tectonics of the Northwestern United States from EarthScope USArray magnetotelluric data: Earth Planetary Science Letters, v. 402, p. 275–289, accessed January 31, 2018, at https://doi.org/10.1016/j.epsl.2013.07.035.

Bedrosian, P.A., and Love, J.J., 2015, Mapping geoelectric fields during magnetic storms—Synthetic analysis of empirical United States impedances: Geophysical Research Letters, v. 42, no. 23, p. 10160–10170, accessed January 31, 2018, at https://doi.org/10.1002/2015GL066636.

Béland, Jean, and Small, Kevin, 2005, Space weather effects on power transmission systems—The cases of Hydro-Québec and Transpower New Zealand Ltd, *in* Daglis, I.A., ed., Effects of space weather on technology infrastructure: Dordrecht, The Netherlands, Springer, p. 287–299, accessed January 31, 2018, at https://doi.org/10.1007/1-4020-2754-0_15.

Blum, Cletus; Love, J.J.; Pedrie, Kolby; Bedrosian, P.A.; and Rigler, E.J., 2015, A one-dimensional model of solid-Earth electrical resistivity beneath Florida: U.S. Geological Survey Open-File Report 2015–1185, 16 p., accessed January 31, 2018, at https://doi.org/10.3133/ofr20151185.

Blum, C.C., White, T.C., Sauter, E.A., Stewart, D.C., Bedrosian, P.A., and Love, J.J., 2017, Geoelectric monitoring at the Boulder magnetic observatory: Geoscientific Instrumentation, Methods and Data Systems, no. 6, p. 447–452.

Bolduc, Léonard, 2002, GIC observations and studies in the Hydro-Québec power system: Journal of Atmospheric and Solar-Terrestrial Physics, v. 64, no. 16, p. 1793–1802, accessed January 31, 2018, at https://doi.org/10.1016/S1364-6826(02)00128-1.

Bonner, L.R., IV, and Schultz, Adam, 2017, Rapid prediction of electric fields associated with geomagnetically induced currents in the presence of three-dimensional ground structure—Projection of remote magnetic observatory data through magnetotelluric impedance tensors: Space Weather, v. 15, no. 1, p. 204–227, accessed January 31, 2018, at https://doi.org/10.1002/2016SW001535.

Borovsky, J.E., Nemzek, R.J., and Belian, R.D., 1993, The occurrence rate of magnetospheric-substorm onsets—Random and periodic substorms: Journal of Geophysical Research, v. 98, no. A3, p. 3807–3813, accessed January 31, 2018, at https://doi.org/10.1029/92JA02556.

Boteler, D.H., 1997, Geomagnetically induced currents, *in* 7th International Symposium on Electromagnetic Compatibility and Electromagnetic Ecology, Saint Petersburg, Russia, June 26–29, 2007, Proceedings: Institute of Electrical and Electronics Engineers, p. 261–264, accessed January 31, 2018.

Boteler, D.H., and Pirjola, R.J., 2017, Modeling geomagnetically induced currents: Space Weather, v. 15, no. 1, p. 258–276, accessed January 31, 2018, at https://doi.org/10.1002/2016SW001499.

Boteler, D.H., Trichtchenko, L., Pirjola, R., Parmelee, J., Souksaly, S., Foss, A., and Marti, L., 2007, Real-time simulation of geomagnetically induced currents: Electromagnetic Compatibility and Electromagnetic Ecology, 7th International Symposium, June 26–29, accessed January 31, 2018, at https://doi.org/10.1109/EMCECO.2007.4371705.

Chave, A.D., 2012, Estimation of the magnetotelluric response function, *in* Chave, A.D., and Jones, A.G., eds., The magnetotelluric method—Theory and practice: Cambridge, United Kingdom, Cambridge University Press, p. 165–218.

Chi, P.J., Engebretson, M.J., Moldwin, M.B., Russell, C.T., Mann, I.R., Hairston, M.R., Reno, M., Goldstein, J., Winkler, L.I., Cruz-Abeyro, J.L., Lee, D.-H., Yumoto, K., Dalrymple, R., Chen, B., and Gibson, J.P., 2013, Sounding of the plasmasphere by Mid-Continent MAgnetoseismic Chain (McMAC) magnetometers: Journal of Geophysical Research—Space Physics, v. 118, no. 6, p. 3077–3086, accessed January 31, 2018, at https://doi.org/10.1002/jgra.50274.

Chulick, G.S., and Mooney, W.D., 2002, Seismic structure of the crust and uppermost mantle of North America and adjacent oceanic basins—A synthesis: Bulletin of the Seismological Society of America, v. 92, no. 6, p. 2478–2492, accessed January 31, 2018, at https://doi.org/10.1785/0120010188.

Connors, M., Russell, C.T., Schofield, I., Hayashi, K., Boteler, D., Asudeh, I., and Irwin, R., 2009, AUTUMN/STEP and POLARIS EHB—Spanning Canada with research magnetometers [abs.]: American Geophysical Union Spring Meeting, Toronto, Canada, May 24–27, no. SM23A-07.

Connors, Martin; Schofield, Ian; Reiter, Kyle; Chi, P.J.; Rowe, K.M.; and Russell, C.T., 2016, The AUTUMNX magnetometer meridian chain in Québec, Canada: Earth Planets Space, v. 68, no. 2, 21 p., accessed January 31, 2018, at https://doi.org/10.1186/s40623-015-0354-4.

Cowley, S.W.H., 2007, Magnetosphere of the Earth, *in* Gubbins, David, and Herrero-Bervera, Emilio eds., Encyclopedia of geomagnetism and paleomagnetism: Dordrecht, The Netherlands, Springer, p. 656–664, accessed January 31, 2018, at https://doi.org/10.1007/978-1-4020-4423-6_205.

Eastwood, J.P., Biffis, E., Hapgood, M.A., Green, L., Bisi, M.M., Bentley, R.D., Wicks, R., McKinnell, L.-A., Gibbs, M., and Burnett, C., 2017, The economic impact of space weather—Where do we stand?: Risk Analysis, v. 37, no. 2, p. 206–218, accessed January 31, 2018, at https://doi.org/10.1111/risa.12765.

Egbert, G.D., 2007a, Robust electromagnetic transfer functions estimates, *in* Gubbins, David, and Herrero-Bervera, Emilio, eds., Encyclopedia of geomagnetism and paleomagnetism: Dordrecht, The Netherlands, Springer, p. 866–870, accessed January 31, 2018, at https://doi.org/10.1007/978-1-4020-4423-6_280.

Egbert, G.D., 2007b, EM modeling, inverse, *in* Gubbins, David, and Herrero-Bervera, Emilio, eds., Encyclopedia of geomagnetism and galeomagnetism: Dordrecht, The Netherlands, Springer, p. 219–223, accessed January 31, 2018, at https://doi.org/10.1007/978-1-4020-4423-6_88.

Engebretson, M.J., Hughes, W.J., Alford, J.L., Zesta, E., Cahill, L.J., Jr., Arnoldy, R.L., and Reeves, G.D., 1995, Magnetometer array for cusp and cleft studies observations of the spatial extent of broadband ULF magnetic pulsations at cusp/cleft latitudes: Journal of Geophysical Research, v. 100, no. A10, p. 19371–19386, accessed January 31, 2018, at https://doi.org/10.1029/95JA00768.

Evans, R.L., 2012, Earth's electromagnetic environment—3A. Conductivity of Earth materials, *in* Chave, A.D. and Jones, A.G., eds., The magnetotelluric method—Theory and practice: Cambridge, United Kingdom, Cambridge University Press, p. 50–95.

Federal Energy Regulatory Commission, 2013, Reliability standards for geomagnetic disturbances: Federal Register, v. 78, no. 100, p. 30747–30762.

Ferguson, I.J., 2012, Instrumentation and field procedure, *in* Chave, A.D., and Jones, A.G., eds., The magnetotelluric method—Theory and practice: Cambridge, United Kingdom, Cambridge University Press, p. 421–479.

Ferguson, I.J., Jones, A.G., and Chave, A.D., 2012, Case histories and geological applications, *in* Chave, A.D., and Jones, A.G., eds., The magnetotelluric method—Theory and practice: Cambridge, United Kingdom, Cambridge University Press, p. 480–544.

Ferguson, I.J., and Odwar, H.D., 1997, Review of conductivity soundings in Canada, appendix 3 *of* Boteler, D.H., ed., Geomagnetically induced currents—Geomagnetic hazard assessment, phase II: Canadian Electricity Association, research report 357 T 848A, prepared by Geological Survey of Canada, v. 3, p. 1–121.

Fernberg, Peter, 2012, One-dimensional earth resistivity models for selected areas of continental United States & Alaska: Electric Power Research Institute Technical Update 1026430, 190 p.

Friedel, R.H.W., Reeves, G.D., and Obara, T., 2002, Relativistic electron dynamics in the inner magnetosphere—A review: Journal of Atmospheric and Solar-Terrestrial Physics, v. 64, no. 2, p. 265–282, accessed January 31, 2018, at https://doi.org/10.1016/S1364-6826(01)00088-8.

Fujii, Ikuko; Ookawa, Takashi; Nagamachi, Shingo; and Owada, Takashi, 2015, The characteristics of geoelectric fields at Kakioka, Kanoya, and Memambetsu inferred from voltage measurements during 2000 to 2011: Earth, Planets and Space, v. 67, no. 62, 17 p., accessed January 31, 2018, at https://doi.org/10.1186/s40623-015-0241-z.

Gannon, J.L., Trichtchenko, L., and Fernberg, P., 2012, United States regional GIC hazard assessment [abs.]: American Geophysical Union Fall Meeting, San Francisco, Calif., December 3–7, no. SM21D–08.

Gill, P., 2009, Electrical power equipment maintenance and testing (2d ed.): Boca Raton, Fla., CRC Press, 1,000 p.

Gjerloev, J.W., 2009, A global ground-based magnetometer initiative: Eos Transactions, American Geophysical Union, v. 90, no. 27, p. 230–231, accessed January 31, 2018, at https://doi.org/10.1029/2009EO270002.

Gonzalez, W.D., Joselyn, J.A., Kamide, Y., Kroehl, H.W., Rostoker, G., Tsurutani, B.T., and Vasyliunas, V.M., 1994, What is a geomagnetic storm?: Journal of Geophysical Research, v. 99, no. A4, p. 5771–5792, accessed January 31, 2018, at https://doi.org/10.1029/93JA02867.

Haines, G.V., and Torta, J.M., 1994, Determination of equivalent current sources from spherical cap harmonic models of geomagnetic field variations: Geophysical Journal International, v. 118, no. 3, p. 499–514, accessed January 31, 2018, at https://doi.org/10.1111/j.1365-246X.1994.tb03981.x.

Hammer, P.T.C., Clowes, R.M., Cook, F.A., Vasudevan, K., and van der Velden, A.J., 2011, The big picture—A lithospheric cross section of the North American continent: GSA Today, v. 21, no. 6, p. 4–10, accessed January 31, 2018, at https://doi.org/10.1130/GSATG95A.1.

Hermance, J.F., 2011, Magnetotelluric interpretation, *in* Gupta, H.K., ed., Encyclopedia of solid earth geophysics: Dordrecht, The Netherlands, Springer, p. 822–829, accessed January 31, 2018, at https://doi.org/10.1007/978-90-481-8702-7.

Holmes, R.R., Jr., Jones, L.M., Eidenshink, J.C., Godt, J.W., Kirby, S.H., Love, J.J., Neal, C.A., Plant, N.G., Plunkett, M.L., Weaver, C.S., Wein, Anne, and Perry, S.C., 2013, U.S. Geological Survey natural hazards science strategy—Promoting the safety, security, and economic well-being of the Nation: U.S. Geological Survey Circular 1383–F, 79 p.

Horton, Randy; Boteler, David; Overbye, T.J.; Pirjola, Risto; and Dugan, R.C., 2012, A test case for the calculation of geomagnetically induced currents: IEEE Transactions on Power Delivery, v. 27, no. 4, p. 2368–2373, accessed January 31, 2018, at https://doi.org/10.1109/TPWRD.2012.2206407.

Joselyn, J.A., and Tsurutani, B.T., 1990, Geomagnetic sudden impulses and storm sudden commencements—A note on terminology: Eos Transactions, American Geophysical Union, v. 71, no. 47, p. 1808–1809, accessed January 31, 2018, at https://doi.org/10.1029/90EO00350.

Kamide, Y., Baumjohann, W., Daglis, I.A., Gonzalez, W.D., Grande, M., Joselyn, J.A., McPherron, R.L., Phillips, J.L., Reeves, E.G.D., Rostoker, G., Sharma, A.S., Singer, H.J., Tsurutani, B.T., and Vasyliunas, V.M., 1998, Current understanding of magnetic storms—Storm-substorm relationships: Journal of Geophysical Research, v. 103, no. A8, p. 17705–17728, accessed January 31, 2018, at https://doi.org/10.1029/98JA01426.

Kappenman, John, 2012, A perfect storm of planetary proportions: IEEE Spectrum, v. 49, p. 26–31.

Kelbert, A., Egbert, G.D., and Schultz, A., 2011, EMTF, magnetotelluric transfer functions: Incorporated Research Institutions for Seismology Data Management Center (IRIS DMC) data services products, accessed January 31, 2018, at https://doi.org/10.17611/DP/EMTF.1.

Kelbert, Anna; Balch, C.C.; Pulkkinen, Antti; Egbert, G.D.; Love, J.J.; Rigler, E.J.; and Fujii, Ikuko, 2017, Methodology for time-domain estimation of storm time geoelectric fields using the 3-D magnetotelluric response tensors: Space Weather, v. 15, no. 7, p. 874–894, accessed January 31, 2018, at https://doi.org/10.1002/2017SW001594.

Kelbert, Anna; Schultz, Adam; and Egbert, Gary, 2009, Global electromagnetic induction constraints on transition-zone water content variations: Nature, v. 460, no. 7258, p. 1003–1006, accessed January 31, 2018, at https://doi.org/10.1038/nature08257.

Kelbert, Anna; Meqbel, Naser; Egbert, Gary D.; and Tandon, Kush, 2014, ModEM—A modular system for inversion of electromagnetic geophysical data: Computers & Geosciences, v. 66, p. 40–53, accessed January 31, 2018, at https://doi.org/10.1016/j.cageo.2014.01.010.

Kihn, E.A., and Ridley, A.J., 2005, A statistical analysis of the assimilative mapping of ionospheric electrodynamics auroral specification: Journal of Geophysical Research, v. 110, A07305, 11 p., accessed January 31, 2018, at https://doi.org/10.1029/2003JA010371.

Lam, Hing-Lan, 2011, From early exploration to space weather forecasts—Canada's geomagnetic odyssey: Space Weather, v. 9, S05004, 5 p., accessed January 31, 2018, at https://doi.org/10.1029/2011SW000664.

Loewe, C.A., and Prölss, G.W., 1997, Classification and mean behavior of magnetic storms: Journal of Geophysical Research, v. 102, no. A7, p. 14209–14213, accessed January 31, 2018, at https://doi.org/10.1029/96JA04020.

Love, J.J., 2008, Magnetic monitoring of Earth and space: Physics Today, v. 61, no. 2, p. 31–37, accessed January 31, 2018, at https://doi.org/10.1063/1.2883907.

Love, J.J., and Bedrosian, P.A., 2018, Extreme-event geoelectric hazard maps, chap. 9 of Buzulukova, N., ed., Extreme events in geospace—Origins, predictability, and consequences: Cambridge, Mass., Elsevier, p. 209–230.

Love, J.J., and Chulliat, Arnaud, 2013, An international network of magnetic observatories: Eos Transactions, American Geophysical Union, v. 94, no. 42, p. 373–374, accessed January 31, 2018, at https://doi.org/10.1002/2013EO420001.

Love, J.J., and Finn, C.A., 2011, The USGS Geomagnetism Program and its role in space weather monitoring: Space Weather, v. 9, S07001, 5 p., accessed January 31, 2018, at https://doi.org/10.1029/2011SW000684.

Love, J.J., and Finn, C.A., 2017, Real-time geomagnetic monitoring for space-weather related applications—Opportunities and challenges: Space Weather, v. 15, p. 820–827, accessed January 31, 2018, at https://doi.org/10.1002/2017SW001665.

Love, J.J., Rigler, E.J, Pulkkinen, Antti, and Balch, C.C., 2014, Magnetic storms and induction hazards: Eos Transactions, American Geophysical Union, v. 95, no. 48, p. 445–446, accessed January 31, 2018, at https://doi.org/10.1002/2014EO480001.

Mann, I.R., Milling, D.K., Rae, I.J., Ozeke, L.G., Kale, A., Kale, Z.C., Murphy, K.R., Parent, A., Usanova, M., Pahud, D.M., Lee, E.-A., Amalraj, V., Wallis, D.D., Angelopoulos, V., Glassmeier, K-H., Russell, C.T., Auster, H.-U., and Singer, H.J., 2008, The upgraded CARISMA magnetometer array in the THEMIS era: Space Science Review, v. 141, no. 1, p. 413–451, accessed January 31, 2018, at https://doi.org/10.1007/s11214-008-9457-6.

Marti, Luis; Rezaei-Zare, Afshin; and Yan, Andrew, 2013, Modelling considerations for the Hydro One real-time GMD management system: Power and Energy Society General Meeting, July 21–25, accessed January 31, 2018, at https://doi.org/10.1109/PESMG.2013.6673069.

Marti, Luis; Yiu, Cynthia; Rezaei-Zare, Afshin; and Boteler, David, 2014, Simulation of geomagnetically induced currents with piecewise layered-Earth models: IEEE Transactions on Power Delivery, v. 29, p. 1186–1193, accessed January 31, 2018, at https://doi.org/10.1109/TPWRD.2014.2317851.

Matsushita, S., 1967, Solar quiet and lunar daily variation fields, *in* Matsushita, S., and Campbell, W.H., eds., Physics of geomagnetic phenomena: New York, Academic Press, v. 1, p. 302–424.

McKay, A.J., and Whaler, K.A., 2006, The electric field in northern England and southern Scotland—Implications for geomagnetically induced currents: IEEE Transactions on Power Delivery, v. 167, no. 2, p. 613–625, accessed January 31, 2018, at https://doi.org/10.1111/j.1365-246X.2006.03128.x.

McLay, S.A., and Beggan, C.D., 2010, Interpolation of externally-caused magnetic fields over large sparse arrays using Spherical Elementary Current Systems: Annales Geophysicae, v. 28, no. 9, p. 1795–1805, accessed January 31, 2018, at https://doi.org/10.5194/angeo-28-1795-2010.

McPherron, R.L., 1991, Physical processes producing magnetospheric substorms and magnetic storms, *in* Jacobs, J.A., ed., Geomagnetism: London, Academic Press, v. 4, p. 593–739.

Menke, W., 2012, Geophysical data analysis—Discrete Inverse Theory, MATLAB Edition: New York, Academic Press, 293 p.

Meqbel, N.M., Egbert, G.D., Wannamaker, P.E., Kelbert, Anna, and Schultz, Adam, 2014, Deep electrical resistivity structure of the northwestern U.S. derived from 3D inversion of USArray magnetotelluric data: Earth and Planetary Science Letters, v. 402, p. 290–304, accessed January 31, 2018, at https://doi.org/10.1016/j.epsl.2013.12.026.

Molinski, T.S., 2002, Why utilities respect geomagnetically induced currents: Journal of Atmospheric and Solar-Terrestrial Physics, v. 64, no. 16, p. 1765–1778, accessed January 31, 2018, at https://doi.org/10.1016/S1364-6826(02)00126-8.

Murphy, B.S., and Egbert, G.D., 2017, Electrical conductivity structure of southeastern North America—Implications for lithospheric architecture and Appalachian topographic rejuvenation: Earth and Planetary Science Letters, v. 462, p. 66–75, accessed January 31, 2018, at https://doi.org/10.1016/j.epsl.2017.01.009.

Nagata, Takesi, 1950, Development of a magnetic storm—The southward shifting of the auroral zone: Journal of Geophysical Research, v. 55, no. 2, p. 127–142, accessed January 31, 2018, at https://doi.org/10.1029/JZ055i002p00127.

National Research Council, 2008, Severe space weather events—Understanding societal and economic impacts, Washington, D.C., The National Academies Press, 144 p., accessed January 31, 2018, at https://doi.org/10.17226/12507.

National Research Council, 2013, Solar and space physics—A science for a technological society: Washington, D.C., National Academies Press, 466 p., accessed January 31, 2018, at https://doi.org/10.17226/13060.

National Science and Technology Council, 2015, National Space Weather Action Plan, Executive Office: Washington, D.C., National Science and Technology Council, 38 p.

Ngwira, Chigomezyo; Pulkkinen, Antti; Bernabeu, Emanuel; Eichner, Jan; Viljanen, Antti; and Crowley, Geoff, 2015, Characteristics of extreme geoelectric fields and their possible causes—Localized peak enhancements: Geophysical Research Letters, v. 42, no. 17, p. 6916–6921, accessed January 31, 2018, at https://doi.org/10.1002/2015GL065061.

Ngwira, C.M., Pulkkinen, Antti, Wilder, F.D., and Crowley, Geoffrey, 2013, Extended study of extreme geoelectric field event scenarios for geomagnetically induced current applications: Space Weather, v. 11, no. 3, p. 121–131, accessed January 31, 2018, at https://doi.org/10.1002/swe.20021.

Nishida, Atsuhiro, 1978, Geomagnetic diagnosis of the magnetosphere: New York, Springer-Verlag, 256 p.

North American Electric Reliability Corporation, 1990, March 13, 1989 geomagnetic disturbance, *in* 1989 system disturbances: Princeton, N.J., North American Electric Reliability Corporation, p. 36–60.

North American Electric Reliability Corporation, 2013, Application guide—Computing geomagnetically induced currents in the bulk-power system: Atlanta, Ga., North American Electric Reliability Corporation, 39 p.

North American Electric Reliability Corporation, 2014a, Transformer thermal impact assessment—Project 2013-03 (Geomagnetic disturbance mitigation): Atlanta, Ga., North American Electric Reliability Corporation, 16 p.

North American Electric Reliability Corporation, 2014b, Benchmark geomagnetic disturbance description: Atlanta, Ga., North American Electric Reliability Corporation, 26 p.

Olsen, Nils, 2007, Natural sources for electromagnetic induction studies, *in* Gubbins, David, and Herrero-Bervera, Emilio, eds., Encyclopedia of geomagnetism and paleomagnetism: Dordrecht, The Netherlands, Springer, p. 696–700, accessed January 31, 2018, at https://doi.org/10.1007/978-1-4020-4423-6_219.

Piccinelli, Roberta, and Krausmann, Elisabeth, 2014, Space weather and power grids—A vulnerability assessment: Luxembourg, European Union, p. 1–53.

Pirjola, Risto, 2002, Review on the calculation of surface electric and magnetic fields and of geomagnetically induced currents in ground-based technological systems: Surveys in Geophysics, v. 23, no. 1, 71 p., accessed January 31, 2018, at https://doi.org/10.1023/A:1014816009303.

Pulkkinen, A., Bernabeu, E., Thomson, A. Viljanen, A., Pirjola, R., Boteler, D., Eichner, J., Cilliers, P.J., Welling, D., Savani, N.P., Weigel, R.S., Love, J.J., Balch, C., Ngwira, C.M., Crowley, G., Schultz, A., Kataoka, R., Anderson, B., Fugate, D., Simpson, J.J., and MacAlester, M., 2017, Geomagnetically induced currents—Science, engineering and applications readiness: Space Weather, v. 15, no. 7, p. 828–856, accessed January 31, 2018, at https://doi.org/10.1002/2016SW001501.

Pulkkinen, A., Pirjola, R., and Viljanen, A., 2008, Statistics of extreme geomagnetically induced current events: Space Weather, v. 6, no. 7, 10 p., S07001, accessed January 31, 2018, at https://doi.org/10.1029/2008SW000388.

Pulkkinen, A., Rastätter, L., Kuznetsova, M., Singer, H., Balch, C., Weimer, D., Toth, G., and Weigel, R., 2013, Community-wide validation of geospace model ground magnetic field perturbation predictions to support model transition to operations: Space Weather, v. 11, no. 6, p. 369–385, accessed January 31, 2018, at https://doi.org/10.1002/swe.20056.

Pulkkinen, Antti; Amm, Olaf; Viljanen, Ari; and BEAR working group, 2003, Ionospheric equivalent current distributions determined with the method of spherical elementary current systems: Journal of Geophysical Research, v. 108, no. A2, p. 117–129, at https://doi.org/10.1029/2001JA005085.

Pulkkinen, Antti; Klimas, Alex; Vassiliadis, Dimitri; Uritsky, Vadim; and Tanskanen, Eija, 2006, Spatiotemporal scaling properties of the ground geomagnetic field variations: Journal of Geophysical Research, v. 111, 15 p., A03305, accessed January 31, 2018, at https://doi.org/10.1029/2005JA011294.

Pulkkinen, Antti, Lindahl, Sture, Viljanen, Ari, and Pirjola, Risto, 2005, Geomagnetic storm of 29–31 October 2003—Geomagnetically induced currents and their relation to problems in the Swedish high-voltage power transmission system: Space Weather, v. 3, no. 8, 19 p., S08C03, accessed January 31, 2018, at https://doi.org/10.1029/2004SW000123.

Qian, Liying; Burns, A.G.; Emery, B.A.; Foster, Benjamin; Lu, Gang; Maute, Astrid; Richmond, A.D.; Roble, R.G.; Solomon, S.C.; and Wang, Wenbin, 2014, The NCAR TIE-GCM—A community model of the coupled thermosphere/ionosphere system, *in* Huba, Joseph; Schunk, Robert; and Khazanov, George, eds., Modeling the ionosphere-thermosphere system: Chichester, United Kingdom, John Wiley & Sons, p. 73–83, accessed January 31, 2018, at https://doi.org/10.1002/9781118704417.ch7.

Rasson, Jean, Toh, Hiroaki, and Yang, Dongmei, 2011, The global geomagnetic observatory network, *in* Mandea, Mioara, and Korte, M.M., eds., Geomagnetic observations and models: New York, Springer, p. 1–25, accessed January 31, 2018, at https://doi.org/10.1007/978-90-481-9858-0_1.

Rastätter, L., Kuznetsova, M.M., Glocer A., Welling D., Meng X., Raeder J., Wiltberger, M., Jordanova, V.K., Yu, Y., Zaharia, S., Weigel, R.S., Sazykin, S., Boynton, R., Wei, H., Eccles, V., Horton, W., Mays, M.L., and Gannon J., 2013, Geospace environment modeling 2008–2009 challenge—D_{st} index: Space Weather, v. 11, no. 4, p. 187–205, accessed January 31, 2018, at https://doi.org/10.1002/swe.20036.

Rigler, E.J., Pulkkinen, A.A., Balch, C.C., and Wiltberger, M.J., 2014, Dynamic geomagnetic hazard maps in space weather operations [abs.]: American Geophysical Union Fall Meeting, San Francisco, Calif., December 15–19, no. SM31A–4178.

Ritter, Oliver, 2007, EM—regional studies, *in* Gubbins, David, and Herrero-Bervera, Emilio, eds., Encyclopedia of geomagnetism and paleomagnetism: Dordrecht, The Netherlands, Springer, p. 242–245, accessed January 31, 2018, at http://doi.org/10.1007/978-1-4020-4423-6.

Rodi, W.L., and Mackie, R.L., 2012, The inverse problem, *in* Chave, A.D., and Jones, A.G., eds., The magnetotelluric method—Theory and practice: Cambridge, United Kingdom, Cambridge University Press, p. 347–420.

Samuelsson, Olof, 2013, Geomagnetic disturbances and their impact on power systems: Lund, Sweden, Industrial Electrical Engineering and Automation, Lund University, 18 p.

Schultz, A., 2010, EMScope—A continental scale magnetotelluric observatory and data discovery resource: Data Science Journal, no. 8, p. IGY6–IGY20, accessed January 31, 2018, at https://doi.org/10.2481/dsj.SS_IGY–009.

Schultz, A., Egbert, G.D., Kelbert, A., Peery, T., Clote, V., Fry, B., Erofeeva, S., and staff of the National Geoelectromagnetic Facility and their contractors, 2006–2018, USArray TA magnetotelluric transfer functions, accessed January 31, 2018, at https://doi.org/10.17611/DP/EMTF/USARRAY/TA.

Schunk, R.W.; Scherliess, Ludger; Sojka, J.J.; Thompson, D.C.; Anderson, D.N.; Codrescu, Mihail; Minter, Cliff; Fuller-Rowell, T.J.; Heelis, R.A., Hairston, Marc; and Howe, B.M., 2004, Global Assimilation of Ionospheric Measurements (GAIM): Radio Science, v. 39, no. 1, RS1S02, accessed January 31, 2018, at https://doi.org/10.1029/2002RS002794.

Simpson, Fiona, and Bahr, Karsten, 2005, Practical magnetotellurics: Cambridge, United Kingdom, Cambridge University Press, 254 p.

Stein, Seth; Stein, Carol; Kley, Jonas; Keller, Randy; Merino, Miguel; Wolin, Emily; Wiens, Douglas; Wysession, M.E.; Al-Equabi, Ghassan; Shen, Weisen; Frederiksen, Andrew; Darbyshire, Fiona; Jurdy, Donna; Waite, G.P.; Rose, W.I.; Vye, Erika; Rooney, Tyrone; Moucha, Robert; and Brown, Eric, 2016, New insights into North America's midcontinental rift: Eos—Earth and Space Science News, no. 97, p. 10–16, accessed January 31, 2018, at https://doi.org/10.1029/2016EO056659.

Stratton, J.A., 1941, Electromagnetic theory: New York, McGraw-Hill Book Company, p. 1–615.

Sun, J., Kelbert, A., and Egbert, G.D., 2015, Ionospheric current source modeling and global geomagnetic induction using ground geomagnetic observatory data: Journal of Geophysical Research, v. 120, no. 10, p. 6771–6796, accessed January 31, 2018, at https://doi.org/10.1002/2015JB012063.

Thomson, A.W.P., 2007, Geomagnetic hazards, *in* Gubbins, David, and Herrero-Bervera, Emilio, eds., Encyclopedia of geomagnetism and paleomagnetism: Dordrecht, The Netherlands, Springer, p. 316–319, accessed January 31, 2018, at https://doi.org/10.1007/978-1-4020-4423-6_117.

Thomson, A.W. P., McKay, A.J., and Viljanen, Ari, 2009, A review of progress in modeling induced geoelectric and geomagnetic fields with special regard to induced currents: Acta Geophysica, v. 57, no. 1, p. 209–219, accessed January 31, 2018, at https://doi.org/10.2478/s11600-008-0061-7.

Torta, J.M., Marcuello, A., Campanyà, J., Marsal, S., Queralt, P., and Ledo, J., 2017, Improving the modeling of geomagnetically induced currents in Spain: Space Weather, v. 15, accessed January 31, 2018, at https://doi.org/10.1002/2017SW001628.

Tóth, Gábor; Meng, Xing; Gombosi, T.I.; and Rastätter, Lutz, 2014, Predicting the time derivative of local magnetic perturbations: Journal of Geophysical Research—Space Physics, v. 119, no. 1, p. 310–321, accessed January 31, 2018, at https://doi.org/10.1002/2013JA019456.

Trichtchenko, L., Fernberg, P.A., and Danskin, D.W., 2016, Geoelectric field modelling for Canadian space weather services: Canadian Geological Survey, Open File 8115, 140 p, accessed January 31, 2018, at https://doi.org/10.4095/299116.

Tsurutani, B.T., and Gonzalez, W.D., 1997, The interplanetary causes of magnetic storms—A review, *in* Tsurutani, B.T.; Gonzalez, W.D.; Kamide, Yohusuke; and Arballo, J.K., eds., Magnetic storms: Washington, D.C., American Geophysical Union, p. 77–89, accessed January 31, 2018, at https://doi.org/10.1029/GM098p0077.

Tsurutani, B.T.; Gonzalez, W.D.; Guarnieri, F.L.; Kamide, Yosuke; Zhou, Xiaoyan; and Arballo, J.K., 2004, Are high-intensity long-duration continuous AE activity (HILDCAA) events substorm expansion events?: Journal of Atmospheric and Solar-Terrestrial Physics, v. 66, no. 2, p. 167–176, accessed January 31, 2018, at https://doi.org/10.1016/j.jastp.2003.08.015.

Unsworth, Martyn, 2007, Magnetotellurics, *in* Gubbins, David, and Herrero-Bervera, Emilio, eds., Encyclopedia of geomagnetism and paleomagnetism: Dordrecht, The Netherlands, Springer, p. 670–673, accessed January 31, 2018, at https://doi.org/10.1007/978-1-4020-4423-6_207.

Valdivia, J.A., Vassiliadis, D., Klimas, A., Sharma, A.S., and Papadopoulos, K., 1999, Spatiotemporal activity of magnetic storms: Journal of Geophysical Research, v. 104, no. A6, p. 12239–12250, accessed January 31, 2018, at https://doi.org/10.1029/1999JA900152.

Viljanen, Ari; Pirjola, Risto; Prácser, Ernö; Katkalov, Juri; and Wik, Magnus, 2014, Geomagnetically induced currents in Europe: Journal of Space Weather and Space Climate, v. 4, no. A09, 9 p., accessed January 31, 2018, at https://doi.org/10.1051/swsc/2014006.

Watermann, J., Rasmussen, O., Stauning, P., and Gleisner, H., 2006, Temporal versus spatial geomagnetic variations along the west coast of Greenland: Advances in Space Research, v. 37, no. 6, p. 1163–1168, accessed January 31, 2018, at https://doi.org/10.1016/j.asr.2005.08.019.

Wei, L.H., Homeier, Nicole, and Gannon, J.L., 2013, Surface electric fields for North America during historical geomagnetic storms: Space Weather, v. 11, no. 8, p. 451–462, accessed January 31, 2018, at https://doi.org/10.1002/swe.20073.

Weidelt, Peter, and Chave, A.D., 2012, The magnetotelluric response function, *in* Chave, A.D., and Jones, A.G., eds. The magnetotelluric method—Theory and practice: Cambridge, United Kingdom, Cambridge University Press, p. 122–164.

Weigel, R.S., 2017, A comparison of methods for estimating the geoelectric field: Space Weather, v. 15, no. 2, p. 430–440, accessed January 31, 2018, at https://doi.org/10.1002/2016SW001504.

Weiss, C.J., 2012, The two- and three-dimensional forward problems, *in* Chave, A.D., and Jones, A.G., eds., The magnetotelluric method—Theory and practice: Cambridge, United Kingdom, Cambridge University Press, p. 303–346.

Weygand, J.M.; Amm, Olaf; Viljanen, A.; Angelopoulos, V.; Murr, D.; Engebretson, M.J.; Gleisner, H.; and Mann, I., 2011, Application and validation of the spherical elementary currents systems technique for deriving ionospheric equivalent currents with the North American and Greenland ground magnetometer arrays: Journal of Geophysical Research, v. 116, no. A3, A03305, 8 p., accessed January 31, 2018, at https://doi.org/10.1029/2010JA016177.

Wilkinson, D., and Heavner, M.J., 2006, Geophysical Institute Magnetometer Array [abs.]: American Geophysical Union Fall Meeting, San Francisco, Calif., December 11–15, no. SA41B–1417.

Williams, M.L., Fischer, K.M., Freymueller, J.T., Tiko, B., Tréhu, A.M., and others, 2010, Unlocking the secrets of the North American continent—An EarthScope Science Plan for 2010–2020: EarthScope, Fairbanks, Alaska, 78 p.

Winch, D.E., 1981, Spherical harmonic analysis of geomagnetic tides, 1964–1965: Philosophical Transactions of the Royal Society of London, Series A, no. 303, p. 1–104, accessed January 31, 2018, at https://doi.org/10.1098/rsta.1981.0193.

Winter, L.M.; Gannon, Jennifer; Pernak, Rick; Huston, Stuart; Quinn, Richard; Pope, Edward; Ruffenach, Alexis; Bernardara, Pietro; and Crocker, Nicholas, 2017, Spectral scaling technique to determine extreme Carrington-level geomagnetically induced currents effects: Space Weather, vol. 15, no. 5, accessed January 31, 2018, at https://doi.org/10.1002/2016SW001586.

Woodroffe, J.R., Morley, S.K., Jordanova, V.K., Henderson, M.G., Cowee, M.M., and Gjerloev, J.G., 2016, The latitudinal variation of geoelectromagnetic disturbances during large (Dst ≤ -100 nT) geomagnetic storms: Space Weather, v. 14, no. 9, p. 668–681, accessed January 31, 2018, at https://doi.org/10.1002/2016SW001376.

Yang, Bo; Egbert, G.D.; Kelbert, Anna; and Meqbel, N.M., 2015, Three-dimensional electrical resistivity of the north-central USA from EarthScope long period magnetotelluric data: Earth and Planetary Science Letters, no. 422, p. 87–93, accessed January 31, 2018, at https://doi.org/10.1016/j.epsl.2015.04.006.

Yoshino, Takashi, 2011, Electrical properties of rocks, *in* Gupta, H.K., ed., Encyclopedia of solid earth geophysics: Dordrecht, The Netherlands, Springer-Verlag, p. 270–276, accessed January 31, 2018, at https://doi.org/10.1007/978-90-481-8702-7_45.

Publishing support provided by the Science Publishing Network,
Denver Publishing Service Center

For more information concerning the research in this report, contact the
Center Director, USGS Geologic Hazards Science Center
Box 25046, Mail Stop 966
Denver, CO 80225
(303) 273-8579

Or visit Geologic Hazards Science Center website at
https://geohazards.cr.usgs.gov/
This publication is available online at
https://doi.org/10.3133/ofr20181043

Love and others—**On the Feasibility of Real-Time Mapping of the Geoelectric Field across North America**—Open-File Report 2018–1043

ISSN 2331-1258 (online)
https://doi.org/10.3133/ofr20181043